International Journal of Pharmaceutics 394 (2010) 60–67

Contents lists available at ScienceDirect

International Journal of Pharmaceutics

journal homepage: www.elsevier.com/locate/ijpharm

Passive asymmetric transport of hesperetin across isolated rabbit cornea

Ramesh Srirangam[a], Soumyajit Majumdar[a,b,*]

[a] Department of Pharmaceutics, School of Pharmacy, The University of Mississippi, University, MS 38677, USA
[b] Research Institute of Pharmaceutical Sciences, School of Pharmacy, The University of Mississippi, University, MS 38677, USA

ARTICLE INFO

Article history:
Received 18 February 2010
Received in revised form 22 April 2010
Accepted 26 April 2010
Available online 9 May 2010

Keywords:
Hesperetin
Hesperidin
Eye
Permeability
Physicochemical
Transcorneal
Asymmetric transport
Transporters
Stability

ABSTRACT

Hesperetin, an aglycone of the flavanone hesperidin, is a potential candidate for the treatment of diabetic retinopathy and macular edema. The purpose of this investigation was to determine solubility, stability and *in vitro* permeability characteristics of hesperetin across excised rabbit corneas. Aqueous and pH dependent solubility was determined using standard shake flask method. Solution stability was evaluated as a function of pH (1.2–9) and temperature (25 and 40 °C). Permeability of hesperetin was determined across the isolated rabbit cornea utilizing a side-bi-side diffusion apparatus, in the apical to basolateral (A–B) and basolateral to apical (B–A) directions. Hesperetin displayed asymmetrical transcorneal transport with a 2.3-fold higher apparent permeability in the B–A direction compared to the A–B direction. The transport process was observed to be pH dependent. Surprisingly, however, the involvement of efflux transporters or proton-coupled carrier-systems was not evident in this asymmetric transcorneal diffusion process. The passive and pH dependent corneal transport of hesperetin could probably be attributable to corneal ultrastructure, physicochemical characteristics of hesperetin and the role of transport buffer components.

1. Introduction

A report from the World Health Organization (WHO) in 2002 estimated that worldwide approximately 161 million people are suffering from visual impairment, out of which 37 million people have blindness and 124 million are suffering from poor vision. Major diseases/disorders responsible for the loss of vision or decreased visual acuity are cataract, glaucoma, diabetic macular edema and diabetic retinopathy (Resnikoff et al., 2004).

Hesperetin is an aglycone of the flavanone glycoside hesperidin and has a molecular formula of $C_{16}H_{14}O_6$ and a molecular weight of 302.27 Da. It is chemically 3′, 5, 7-trihydroxy-4′-methoxy flavanone (Fig. 1) and is obtained by acid hydrolysis of hesperidin. In recent years, researchers have reported various pharmacological properties of hesperetin, in addition to that of its glycoside, hesperidin. Hesperetin can act as a potential antioxidant (Choi, 2008; Hwang and Yen, 2008), can increase the ocular blood flow and minimize ischemic injury to the retina (Chiou and Xu, 2004), can decrease vascular permeability (Paysant et al., 2008; Garg et al., 2001) and act as a neuroprotectant (Choi and Ahn, 2008; Hwang and Yen, 2008), anti-inflammatory agent (Hirata et al., 2005; Galati et al., 1994) and anticancer agent (Aranganathan et al., 2009, 2008). Importantly, as described in earlier reports (Majumdar and Srirangam, 2009), some of the pharmacological activities of hesperidin and hesperetin may be very useful in the prevention and/or treatment of certain eye diseases/disorders such as diabetic retinopathy, diabetic macular edema and cataract.

In order for a drug to be effective in the treatment of ocular diseases, therapeutic concentrations need to be achieved and maintained at the target site. Ocular drug levels may be achieved through topical, periocular, intravitreal, systemic or oral administration. Following administration, the therapeutic moiety has to cross the relevant ocular physiological barriers like the cornea, sclera, choroid and retinal pigmented epithelium (RPE), depending on the route of drug application and the target site. To diffuse across these ocular tissues, the drug molecule should demonstrate adequate permeability characteristics, which in turn depends on the physicochemical properties of the compound.

Hesperetin has been reported to be a substrate of efflux proteins as well as proton dependent influx transporters, although there are conflicting reports (Brand et al., 2008; Kobayashi et al., 2008; Mertens-Talcott et al., 2007; Serra et al., 2008). The corneal tissue is reported to express several efflux transporters such as P-glycoprotein (P-gp), multi-drug resistant proteins (MRP) and breast cancer resistant proteins (BCRP) (Mannermaa et al., 2006; Vellonen et al., 2010). Additionally, peptide transporters, amino acid transporters, monocarboxylic acid transporters (MCTs) are amongst the identified influx transporters present on the corneal epithelium

* Corresponding author at: Department of Pharmaceutics, The University of Mississippi, 111 Faser Hall, University, MS 38677, USA. Tel.: +1 662 915 3793; fax: +1 662 915 1177.
E-mail address: majumso@olemiss.edu (S. Majumdar).

0378-5173/$ – see front matter © 2010 Elsevier B.V. All rights reserved.
doi:10.1016/j.ijpharm.2010.04.036

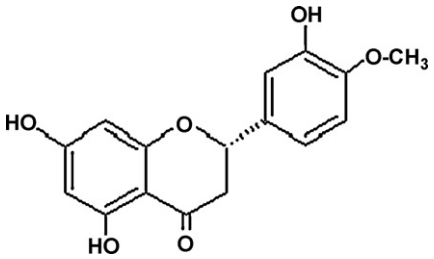

Fig. 1. Chemical structure of hesperetin (3′,5,7-trihydroxy-4′-methoxy flavanone).

(Mannermaa et al., 2006). Incidentally one report suggested the involvement of an MCT type transporter in the transcellular transport of hesperetin (Kobayashi et al., 2008). The current project was undertaken to evaluate the *in vitro* permeability characteristics of hesperetin across the isolated rabbit cornea. Additionally, solubility, stability and physicochemical properties of hesperetin were also determined.

2. Materials and methods

2.1. Materials

Hesperetin, verapamil, MK-571, erythromycin and 2-hydroxypropyl beta cyclodextrin (HP-β-CD) (1300 MW 0.6 substitution) were purchased from Sigma–Aldrich (St. Louis, MO, USA). Sodium azide, oubain, probenecid, 2,4,-dinitrophenol (2,4-DNP) were obtained from Fisher Scientific (Fairlawn, NJ, USA). All other solvents and chemicals were also purchased from Fisher Scientific (Fairlawn, NJ, USA) and used as such.

2.2. Ocular tissues

Corneas were isolated from euthanized adult male, albino, New Zealand rabbits weighing between 2 and 2.5 kg (Myrtle's Rabbitry, Thompson Station, TN, USA). All experiments using rabbits conformed to the Association of Research in Vision and Ophthalmology (ARVO) statement on the use of Animals for use in Ophthalmic and Vision Research.

2.3. Solubility studies

Aqueous solubility of hesperetin was determined using the standard shake flask method wherein an excess quantity of drug was added to 5 mL of the solvent in tightly capped glass vials. Samples were constantly agitated at 75 rpm, at room temperature (25 °C), for 24 h in a reciprocating water bath (Fisher Scientific, USA) for uniform mixing. At the end of 24 h, samples were centrifuged (AccuSpin 17R, Fisher Scientific, USA) and the supernatant was aliquoted and analyzed for drug content. Solubility was determined in distilled water and in buffers (pH 1.3–9) prepared following procedures described in the United States Pharmacopoiea. Additionally, effect of surfactants (Tween® 80, Cremophor® EL, D-alpha-tocopheryl polyethylene glycol 1000 succinate (Vitamin E-TPGS) and sodium lauryl sulphate; all at 1%, w/v concentration) and HP-β-CD on the solubility of hesperetin was evaluated. HP-β-CD concentrations used for the phase solubility studies were 1% (w/v), 2.5% (w/v), 5% (w/v), 7.5% (w/v), 10% (w/v), 15% (w/v) and 20% (w/v) in water.

2.4. Solution stability

Stability of hesperetin in aqueous solution was determined at various pH (1.3, 3, 5, 7.4 and 9) and temperature (25 and 40 °C) conditions. Buffers were prepared following USP procedures. Stability studies were initiated with the addition of hesperetin stock solution to 5 mL of the respective buffer previously equilibrated to either 25 or 40 °C. The final concentrations of hesperetin in these solutions were 5 μg/mL. Aliquots (200 μL) were collected at predetermined time points and were stored at −80 °C until further analysis. Samples were analyzed using HPLC technique as described under Section 2.7.

2.5. Log P and pK_a

Predicted value of log *P* and pK_a were obtained using ACD/I-Lab Web Service (ACD/log *P* 8.02) and (ACD/pK_a 8.03), respectively.

2.6. Transcorneal permeation experiments

Experiments were performed following previously described procedures (Majumdar and Srirangam, 2009). Briefly, studies were carried out using a side-bi-side diffusion apparatus (PermeGear Inc., USA). Rabbits were euthanized with an overdose of sodium pentobarbital injected through the marginal ear vein. Eyes were collected immediately and washed with dulbecco's phosphate buffer saline (DPBS) and the corneas were isolated with a ring of sclera around it, to help in mounting between the diffusion cells. Corneas were washed in DPBS and mounted on the side-bi-side diffusion apparatus (standard 9 mm cells were used) with the epithelial side facing the donor cell for apical to basolateral transport (A–B) and with the endothelial side facing the donor cell for basolateral to apical transport (B–A). Temperature of the cells was maintained at 34 °C with the help of a circulating water bath. In all cases, unless otherwise mentioned, 3 mL of transport buffer (DPBS, pH 7.4, containing 0.5% (w/v) HP-β-CD) or drug solution (150 μM hesperetin in DPBS, pH 7.4 or 6, with 0.5%, w/v HP-β-CD) was added to the apical side of the cornea while 3.2 mL of the drug solution or transport buffer, respectively, was added to the basal side, to maintain the natural hydrostatic pressure. Aliquots (200 μL) were removed at predetermined time points (15, 30, 45, 60, 90, 120, 150 and 180 min) from the receiver side and the volume withdrawn was replaced with an equal volume of transport buffer. Samples were stored at −80 °C until further analysis.

2.6.1. pH dependent transport

Donor solution pH was decreased to 6 from 7.4 using dilute HCl solution. Effect of pH on transcorneal diffusion was evaluated in both A–B and B–A directions.

2.6.2. Inhibition experiments

Hesperetin's corneal permeation was determined in the presence of inhibitors of various transport systems. Permeation of hesperetin in the A–B direction was studied in the presence of 100 μM verapamil, 100 μM erythromycin, 500 μM 2,4-DNP, 1 mM sodium azide and 1 mM ouabain. Transport in the B–A direction was carried out in the presence of 100 μM verapamil, 100 μM erythromycin, 50 μM chrysin, 1 mM probenecid, 50 μM MK 571, 1 mM sodium azide and 1 mM ouabain. In the studies using sodium azide and ouabain, corneas were presoaked in the respective transport media (with inhibitors but no drug) for 30 min before the initiation of the transport studies. Transcorneal permeation of hesperetin, in A–B direction, in the presence of 2,4-DNP transport was studied across a pH gradient, with the donor solution pH adjusted to 6 and the receiver solution pH at 7.4.

2.6.3. Concentration dependent transport

Permeation of hesperetin in the A–B direction as a function of drug concentration (from 25 to 500 μM) was determined.

Transcorneal permeation protocols as described earlier were followed.

2.6.4. Transcorneal permeation in the presence of Tween® 80

To see the effect of components of transport medium on asymmetrical transport of hesperetin, transcorneal permeation was carried out in the presence of 0.25% (w/v) and 0.5% (w/v) Tween® 80 in DPBS (pH 7.4), instead of HP-β-CD, in both A–B and B–A directions, respectively. Transcorneal permeation protocols as described earlier were followed.

2.6.5. Corneal integrity

In order to ascertain that the integrity of the corneas were maintained under the experimental conditions employed, control studies were carried out using acyclovir (ACV; 1 mM), as a marker compound. Corneal permeability, both A–B and B–A, of ACV was determined in the presence of hesperetin and components of the transport medium (0.5% HP-β-CD or Tween® 80). In these studies samples were analyzed for both ACV and hesperetin content and the transcorneal permeability values for both were determined.

2.7. Analytical method

Hesperetin content in the samples was estimated using an analytical method based on reversed phase HPLC. An HPLC system equipped with Waters 600 pump controller, 2470 dual wavelength UV detector, refrigerated 717 plus auto-sampler and Agilent 3394B integrator was used. The detector was operated at 284 nm. Mobile phase consisted of 20 mM monobasic potassium phosphate (pH adjusted to 2.5 with orthophosphoric acid) and acetonitrile in a ratio of 50:50 and the flow rate was maintained at 1 mL/min. A Waters Symmetry Shield C18 column was used. ACV content was determined following previously published methods (Majumdar et al., 2010).

2.8. Data analysis

Parameters associated with drug diffusion across the cornea like rate, flux and apparent permeability coefficient were calculated following previously described methods (Majumdar and Srirangam, 2009). Briefly, steady state (SS) fluxes (μg/min/cm^2) were determined from the slope of the cumulative amount of drug (M) transported vs. time (t) graph and expressed as per unit of surface area (A) as described by Eq. (1):

$$\text{Flux}\,(J) = \frac{\mathrm{d}M/\mathrm{d}t}{A} \quad (1)$$

Membrane permeability (cm/s) values were determined by normalizing the steady state fluxes to the donor concentration C_d according to Eq. (2).

$$\text{permeability}\,(P_{app}) = \frac{\text{flux}}{C_d} \quad (2)$$

Statistical analysis was carried using JMP software (Version 5.0.1). ANOVA was used to see the difference among different groups and a Student's t-test for the difference between two groups. A p value less than 0.05 is considered statistically significant.

3. Results

3.1. Solubility studies

Saturation solubility of hesperetin in water was found to be 15.72 ± 0.58 μg/mL and was pH dependent. Solubility increased with an increase in solution pH. Presence of surfactants also improved hesperetin's aqueous solubility. Solubility of hesperetin in water, various buffers and surfactant solutions are presented in Table 1.

Table 1
Saturation solubility of hesperetin in water, buffers (200 mM) and surfactant solutions (1%, w/v). Samples were kept under constant agitation for 24 h at 25 °C in a shaking water bath. Values are represented as mean ± SD (n = 3).

Solvent	Saturation solubility (μg/mL)
Water	15.72 ± 0.58
Buffer (pH 1.3)	8.56 ± 1.31
Buffer (pH 3.0)	11.32 ± 0.60
Buffer (pH 5.0)	9.33 ± 1. 31
Buffer (pH 7.4)	19.58 ± 3.32
Buffer (pH 9.0)	500.26 ± 69.75
Tween® 80 solution	269.21 ± 10.92
Cremophor® EL solution	255.21 ± 64.68
D-Alpha-tocopheryl polyethylene glycol 1000 succinate (Vitamin E-TPGS) solution	340.49 ± 19.65
Sodium lauryl sulphate (SLS) solution	300.82 ± 16.80

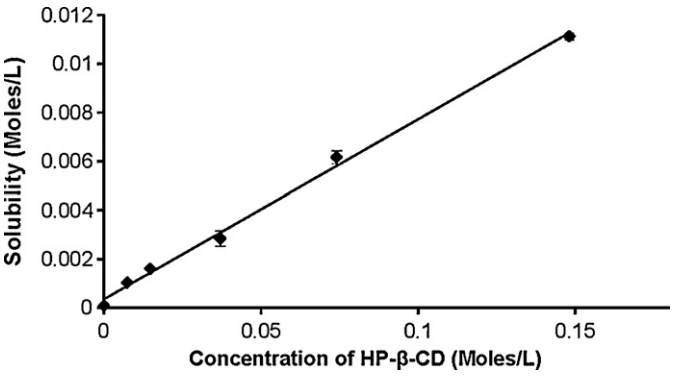

Fig. 2. Phase solubility of hesperetin in the presence of 2-hydroxypropyl beta cyclodextrin (HP-β-CD). The study was carried out at a temperature of 25 °C for 24 h. Values are represented as mean ± SD (n = 3).

Hesperetin's solubility was dramatically increased in the presence of HP-β-CD. Phase solubility studies were conducted as a function of increasing concentrations of HP-β-CD. A plot of HP-β-CD concentration against the saturation solubility of hesperetin yielded an A_L type phase solubility curve (Fig. 2). Association constant (K), complexation efficiency (CE) and regression coefficient (R^2) were found to be 991 ± 4 M^{-1}, 0.079 ± 0.005 and 0.9953 ± 0.0043, respectively.

3.2. Stability in aqueous solutions

Aqueous solution stability was tested as a function of pH and temperature. Hesperetin was observed to be stable in pH 1.2, 3 and 5 buffers for 3 months (last time point tested). However, apparent first order degradation was observed in pH 7.4 and 9 solutions and the degradation rates were temperature dependent. The apparent first order degradation rate constants (K) and estimated half-lives are presented in Table 2.

Table 2
Solution stability of hesperetin as a function of pH and temperature. Values are represented as mean ± SD (n = 3).

pH	Temperature (°C)	K (day^{-1})	$t_{1/2}$ (days)
7.4	25	0.010 ± 0.0003	72 ± 2
7.4	40	0.041 ± 0.0007	17 ± 0.3
9	25	0.021 ± 0.0007	34 ± 1
9	40	0.121 ± 0.012	6 ± 0.6

Table 3
Apparent permeability coefficients of hesperetin across the isolated rabbit cornea. Transport was carried out in a side-bi-side diffusion apparatus at a temperature of 34 °C. Donor solution contained 150 μM hesperetin. Values are represented as mean ± SD ($n = 4$).

Direction and pH of diffusion media	Apparent permeability coefficient ($\times 10^{-6}$ cm/s)
Apical (pH 7.4) to basolateral (pH 7.4) direction	4.31 ± 0.73
Basolateral (pH 7.4) to apical (pH 7.4) direction	10.12 ± 1.92
Apical (pH 6.0) to basolateral (pH 7.4) direction	16.65 ± 3.72
Basolateral (pH 6.0) to apical (pH 7.4) direction	15.89 ± 3.38

3.3. Log P and pK_a

Using ACD/log *P* and ACD/pK_a softwares, hesperetin's log *P* was estimated to be 2.90 ± 0.39 and pK_a values were calculated to be 9.65, 8.5 and 7.55 for the hydroxyl groups positioned at 3′, 5 and 7, respectively.

3.4. Transcorneal permeability

3.4.1. Transport in the apical to basolateral (A–B) and the basolateral to apical (B–A) directions

Hesperetin's apparent permeability coefficients across the isolated rabbit cornea are presented in Table 3. In this case, both donor and receiver chamber pH was maintained at 7.4. Apparent permeability of hesperetin in the B–A direction was significantly higher, by about 2.3-fold, than that in the A–B direction.

3.4.2. Inhibition studies

Asymmetric transport of hesperetin across the cornea, in the absence of a proton gradient, could be due to the involvement of influx/efflux transporters. In order to establish/identify the involvement of a carrier system, hesperetin transport was carried out in the presence of inhibitors/substrates of various nutrient transporters. The pH of the receiver and donor chamber solutions were maintained at 7.4. Verapamil (a known P-gp substrate) or erythromycin (a known P-gp/MRP inhibitor), did not produce a significant difference in the permeability of hesperetin, in either direction. The metabolic inhibitors ouabain (a Na^+/K^+ ATPase inhibitors) and sodium azide (an uncoupler of oxidative phosphorylation) also did not demonstrate any effect on the transcorneal permeation of hesperetin. Additionally, B–A transport of hesperetin was studied in the presence of inhibitors of other nutrient transport systems. MK571 (a specific MRP inhibitor), chrysin (a specific BCRP inhibitor) or probenecid (a specific OCT inhibitor) did not effect transcorneal hesperetin permeability. Furthermore, diffusion in the B–A direction was studied in a sodium free media, to check for the involvement of a sodium dependent transporter. In this case also a significant change in apparent permeability was not observed (Figs. 3 and 4).

3.4.3. pH dependent transport

Donor solution pH was decreased from 7.4 to 6, and transport was evaluated in both A–B and B–A directions. In the presence of a proton gradient, hesperetin exhibited a higher apparent permeability in both A–B (a 4-fold increase) and B–A (a 1.5-fold increase) directions, compared to its apparent permeability in the absence of a proton gradient (donor and receiver solution pH 7.4) in the A–B and B–A directions (Table 3). Since, hesperetin demonstrated greater permeability in the presence of a proton gradient, transport studies were repeated in the presence of a protonophore, 2,4-DNP. A significant change in transcorneal hesperetin transport was however, not evident.

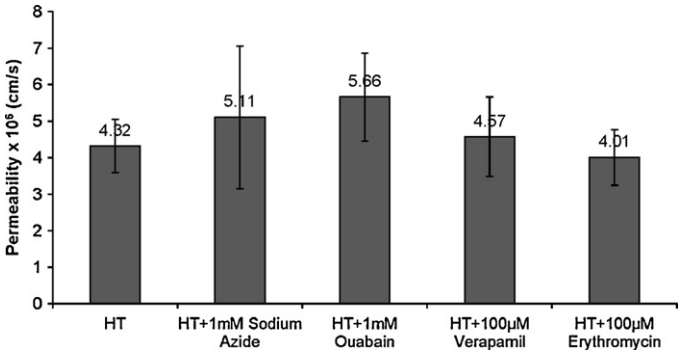

Fig. 3. Transcorneal permeability of hesperetin (HT) (150 μM) in the apical to basolateral (A–B) direction alone and in the presence of various drug transporter inhibitors. Values are represented as mean ± SD ($n = 4$). A statistically significant difference was not observed between the permeability of hesperetin alone and in the presence of drug transporter inhibitors.

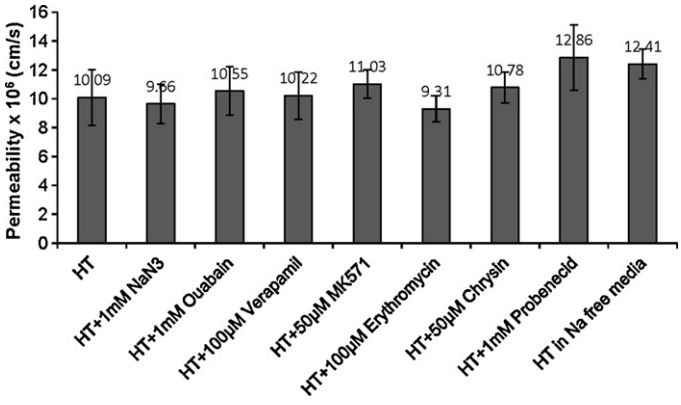

Fig. 4. Transcorneal permeability of hesperetin (HT) (150 μM) in the basolateral to apical (B–A) direction alone and in the presence of various drug transporter inhibitors and in a sodium free media. Values are represented as mean ± SD ($n = 4$). A statistically significant difference was not observed between the permeability of hesperetin alone and in the presence of drug transporter inhibitors.

3.4.4. Concentration dependent transport

Hesperetin's transport in the A–B direction as a function of donor concentration was studied to further investigate the asymmetrical transport characteristics. Both donor and receiver solution pH was maintained at pH 7.4. A linear increase in the flux with an increasing concentration of hesperetin was observed in the concentration range tested (Fig. 5).

3.4.5. Transcorneal permeation in the presence of Tween® 80

Hesperetin's apparent permeability coefficients across the cornea in the presence of 0.25% (w/v) Tween® 80 were

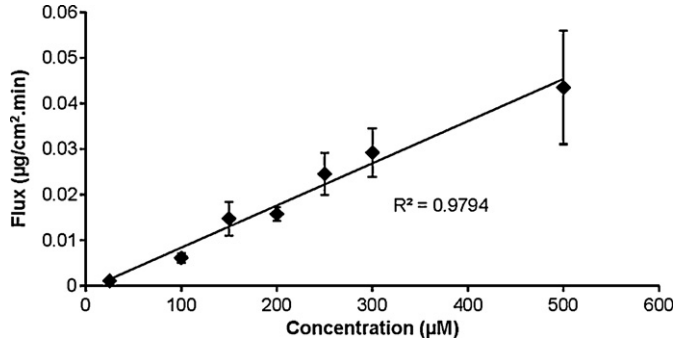

Fig. 5. Concentration dependent transcorneal flux of hesperetin in the apical to basolateral (A–B) direction. Values are represented as mean ± SD ($n = 4$).

found to be $5.37 \pm 1.3 \times 10^{-6}$ and $7.85 \pm 1.6 \times 10^{-6}$ cm/s in the A–B and B–A directions, respectively. In the presence of 0.5% (w/v) Tween® 80 apparent permeability coefficients were found to be $2.80 \pm 0.6 \times 10^{-6}$ cm/s in the A–B direction and $3.60 \pm 0.8 \times 10^{-6}$ cm/s in the B–A direction. Thus, in the presence of 0.25% and 0.5% w/v Tween® 80, a 1.5- and 1.3-fold difference, respectively, exists between the A–B and B–A apparent permeability values.

3.4.6. Corneal integrity

Corneal permeability of ACV in plain DPBS was observed to be $2.86 \pm 0.86 \times 10^{-6}$ and $3.28 \pm 0.91 \times 10^{-6}$ cm/s in the A–B and B–A directions, respectively. The difference in the permeability values was not statistically different. In the presence of hesperetin and HP-β-CD or hesperetin and Tween® 80, a significant difference between the A–B and B–A permeability values of ACV was also not evident, indicating that the corneal integrity was not compromised under the experimental conditions employed. While ACV did not show any difference in the A–B and B–A corneal permeability values, a significant difference (2.3- and 1.4-fold in the presence of HP-β-CD and Tween® 80, respectively) was observed with respect to the corneal permeability of hesperetin.

4. Discussion

Hesperetin has the potential to treat multiple ocular diseases like diabetic retinopathy, diabetic macular edema and cataract, by virtue of its wide-ranging pharmacological activities (Chiou and Xu, 2004; Choi, 2008; Choi and Ahn, 2008; Hwang and Yen, 2008). However, drug delivery to the eye is a challenging task and successful ophthalmic formulation development requires an understanding of the physicochemical and permeability characteristics of a drug molecule. The current research project was undertaken to delineate the *in vitro* permeation profile of hesperetin across isolated rabbit corneal tissue.

Hesperetin demonstrated very poor aqueous solubility and exhibited a pH dependant solubility profile. While a significant difference in solubility was not observed in the acidic pH range (1.3, 3 and 5), under alkaline conditions solubility increased with an increase in solution pH (Table 1). Hesperetin possesses three phenolic hydroxyl groups (Fig. 1) and thus behaves like a weak acid. However, all the predicted pK_a values are above 7.5, suggesting hesperetin will dissociate under alkaline pH conditions. Consistent with this, higher aqueous solubility was observed in the basic pH range. Presence of HP-β-CD significantly increased aqueous solubility of hesperetin and this is in agreement with earlier reports (Tommasini et al., 2005). A linear increase in solubility with increasing concentrations of HP-β-CD (Fig. 2) indicates that HP-β-CD is probably forming a 1:1 molar complex with hesperetin. From the phase solubility studies, the complexation efficiency for hesperetin and HP-β-CD was found to be relatively high compared to hesperidin (Majumdar and Srirangam, 2009), its parent compound. This could be due to the much higher lipophilicity of hesperetin ($\log P$ 2.9) compared to hesperidin ($\log P$ 1.78). Hesperetin was found to be stable in the acidic buffers (pH 1.2–5). However, hesperetin's concentration was found to decrease with time with an increase in solution pH and temperature (pH 7.4–9) (Table 2).

Transcorneal diffusion of hesperetin was studied using an *in vitro* side-bi-side diffusion apparatus. The studies were carried out using DPBS (pH 7.4) containing 0.5% (w/v) HP-β-CD as the transport medium. Hesperetin exhibited asymmetric permeability across the isolated rabbit cornea, with the apparent permeability in the B–A direction being 2.3-fold greater than that in the A–B direction. Higher B–A apparent permeability could indicate the involvement of the efflux transporters (e.g. MRP, P-gp and BCRP) expressed on the corneal epithelium (Mannermaa et al., 2006; Vellonen et al., 2010). Earlier studies, however, present confounding evidence with respect to the interaction of hesperetin with efflux transporters (Brand et al., 2008, 2010; Kobayashi et al., 2008; Serra et al., 2008). Kobayashi et al. (2008) demonstrated that a proton-coupled and energy dependent transporter was responsible for this higher A–B flux across the Caco-2 cells. Other researchers, however, reported symmetrical transport of hesperetin across Caco-2 cells (Serra et al., 2008) and that hesperetin's A–B transport was unaltered in the presence of specific inhibitors of different ABC transporters, signifying that hesperetin moves through the Caco-2 cell monolayer by passive diffusion (Brand et al., 2008, 2010).

In the current study, the apparent transcorneal permeability profile of hesperetin suggested possible involvement of efflux transporters in the permeation process. However, a significant increase in the A–B transport of hesperetin in the presence of verapamil and erythromycin (P-gp and MRP inhibitors) or sodium azide and ouabain (metabolic inhibitors) was not evident (Fig. 3). To further investigate the role of influx drug transporters in hesperetin's asymmetric transcorneal transport, B–A transport was studied in the presence of verapamil, erythromycin, MK-571 (P-gp/MRP inhibitors), probenecid (OATP inhibitor), chrysin (BCRP inhibitor), sodium azide and ouabain. Hesperetin's B–A transport remained unaltered in all cases (Fig. 4). These results suggest that the B–A diffusion of hesperetin is not facilitated by any of the transporters tested and that the transport process is energy and sodium independent since both sodium azide and ouabain produced an insignificant effect on transcorneal drug transport. Moreover, transporter involvement typically yields a curvilinear or saturable concentration dependent flux. However, in the present study, transcorneal hesperetin flux, in the A–B direction, increased linearly with increasing concentrations of hesperetin (Fig. 5), within the concentration range tested. The above results, taken together, strongly suggest that corneal influx/efflux transporters do not interact with hesperetin and are not responsible for the observed asymmetric transcorneal transport of hesperetin.

It is evident from the pH dependent solubility studies and the pK_a value (9.65, 8.5 and 7.55) of the drug molecule, that hesperetin undergoes ionization and would thus exhibit pH dependent permeability rates. To evaluate the effect of ionization on transcorneal hesperetin permeability, the studies were repeated with the donor solution pH adjusted to 6. The receiver solution pH was maintained at 7.4. This resulted in a significant increase in hesperetin's apparent permeability in both A–B and B–A directions (Table 3), although the increase in the A–B direction was significantly greater than the increase in the B–A direction. At a lower pH value (pH 6), greater than 95% of the drug exists in the unionized state (pK_a 7.55), which would explain the higher permeability of hesperetin. The higher A–B flux of the drug could also be because of a proton-coupled transporter. However, in the presence of a protonophore, 2,4-DNP, a significant change in the apparent A–B permeability was not evident, eliminating the involvement of a proton-coupled carrier system.

To evaluate the effect of the transport medium (especially HP-β-CD), apparent transcorneal permeability of hesperetin was evaluated using DPBS (pH 7.4) containing 0.25% (w/v) or 0.5% (w/v) Tween® 80 instead of HP-β-CD. Transport in the B–A direction was 1.5- and 1.3-fold higher compared to the A–B direction, in the presence of 0.25% (w/v) and 0.5% (w/v) Tween® 80, respectively. This study further supports the observation that transport of hesperetin across the rabbit cornea is asymmetrical, especially at lower concentrations of the surfactant. Transcorneal permeability coefficient of hesperetin in the presence of 0.25% (w/v) Tween® 80 was 2-fold greater than that in the presence of 0.5% (w/v) Tween® 80. This is probably because of increased micellar entrapment of the drug (same drug concentration but increased surfactant levels).

This is consistent with other studies reporting a decrease in apparent permeability with increasing surfactant concentration (Chiu et al., 2003).

Considering, hesperetin exhibits asymmetrical transport across the rabbit cornea in the absence of a proton gradient and symmetrical transport in the presence of a proton gradient and that the corneal influx or efflux transporters are not involved in the process, the following hypothesis could probably explain the observed results. Figs. 6 and 7 illustrate the theory schematically.

The three physical barriers associated with transcorneal diffusion are the epithelium, the stroma and the endothelium. Drug transport across these different corneal layers can be represented by Fick's first law of diffusion.

According to Fick's first law of diffusion:

$$\frac{dM}{dt} = \frac{DSK_p(C_d - C_r)}{h} \quad (4)$$

where dM/dt is the mass transfer rate, D is the diffusion coefficient, S is the surface area, K_p is the apparent partition coefficient, C_d is the concentration of hesperetin in the donor compartment, C_r is the concentration of hesperetin in the receiving compartment ($C_d - C_r$) is the concentration gradient and h is the membrane or barrier thickness.

Consider, 'DSK_p/h' as K' and ($C_d - C_r$) equals C_d (as $C_d \gg C_r$). When hesperetin is permeating in the A–B direction, the net mass transfer rate can be described by Eq. (5):

$$\frac{dM}{dt}(A-B) = K_1[C_{UI}]_{Dn} + K_2[C_I]_{Dn} + K_3[C_{UI}]_{Ep} + K_4[C_{UI}]_{St} + K_5[C_I]_{St} + K_6[C_{UI}]_{End} \quad (5)$$

where K_1, K_2,... and K_6 are the rate constants associated with the diffusion of the drug; $[C_{UI}]$ represents concentration of unionized hesperetin; $[C_I]$ represents concentration of ionized hesperetin. The subscripts Dn, Ep, St and End represent concentration of the drug in donor chamber, corneal epithelial cells, corneal stroma and corneal endothelial cells, respectively.

Hesperetin is known to cross biological barriers by both paracellular as well as transcellular pathways (Brand et al., 2008). In the A–B direction, the corneal epithelium, comprised of multiple layers of epithelial cells packed tightly together, is the first barrier encountered. When the donor solution is maintained at pH 7.4, hesperetin (pK_a 7.55) exists in both the unionized (UI) and ionized (I) states and only the unionized fraction would diffuse transcellularly into the epithelial cells (represented by $K_1[C_{UI}]_{Dn}$ of Eq. (5)). Paracellular diffusion of the ionized form (represented by $K_2[C_I]_{Dn}$ of Eq. (5)) would be negligible due to the presence of the corneal epithelial tight junctions. A fraction of the unionized hesperetin diffusing into the corneal epithelial cells, then partitions out into the stroma, which is composed of about 90% water (represented by $K_3[C_{UI}]_{Ep}$ of Eq. (5)). In view of the fact that the log P of hesperetin is 2.9, it is reasonable to conclude that the diffusivity (D) of the drug across the epithelial cell membrane into the stroma will be very low and thus only a very small fraction of the unionized hesperetin would partition into the stroma from the epithelial layer (i.e. $K_3[C_{UI}]_{Ep}$ will be very low). Equilibrium between the ionized and unionized fractions would be established in the stroma (pH 7.2–7.4). From the stroma the unionized fraction of hesperetin would move into the endothelial cell membrane at a rate represented by K_4 $[C_{UI}]_{St}$ of Eq. (5). Ionized hesperetin, a small molecule, can also diffuse from the stroma across the intercellular junctions of the corneal endothelial cell layer (represented by $K_5[C_I]_{St}$ of Eq. (5)), which are leaky in nature (Prausnitz and Noonan, 1998), into the receiver solution. The final component of the overall diffusion process would be the movement of drug into the receiver solution from the endothelial cells (represented by $K_6[C_{UI}]_{End}$ of Eq. (5)) which would be facilitated by, HP-β-CD or Tween® 80, solubilizing components of the receiver solution.

Thus, with respect to transcorneal A–B transport, the epithelial tight junctions, blocking the diffusion of ionized hesperetin ($K_2[C_I]_{Dn}$), and poor partitioning of the unionized hesperetin from the corneal epithelial layer into the stroma ($K_3[C_{UI}]_{Ep}$) act as the rate limiting steps in the transcorneal diffusion process. The above is schematically represented in Fig. 6.

On the other hand when hesperetin is diffusing in the B–A direction, the net mass transfer rate can be described by Eq. (6):

$$\frac{dM}{dt}(B-A) = K_7[C_{UI}]_{Dn} + K_8[C_I]_{Dn} + K_9[C_{UI}]_{End} + K_{10}[C_{UI}]_{St} + K_{11}[C_I]_{St} + K_{12}[C_{UI}]_{Ep} \quad (6)$$

where K_7, K_8, ...and K_{12} are the rate constants associated with diffusion of the drug. This has been schematically described in Fig. 7.

In the B–A direction the endothelial cells do not present a formidable barrier to the diffusion of the unionized (represented by $K_7[C_{UI}]_{Dn}$ of Eq. (6)) or ionized (represented by $K_8[C_I]_{Dn}$ of Eq. (6)) hesperetin fractions into the corneal stroma because of a decreased transcellular diffusion length (single layered endothelial cells compared to the multilayered corneal epithelium) and the lack of endothelial cell tight junctions, respectively. This is consistent with several studies that demonstrate transport across the corneal endothelial cells is much higher than that across the epithelial cells for several drugs (Prausnitz and Noonan, 1998). In the stroma, since the pH is 7.4, equilibrium between the ionized and unionized hesperetin fractions is established. Considering the less restricted access of the ionized form to the stroma in the B–A direction, stromal hesperetin concentrations will be significantly higher than that achieved in the A–B direction:

$$(([C_{UI}] + [C_I])_{St})_{B-A} \gg (([C_{UI}] + [C_I])_{St})_{A-B} \quad (7)$$

The unionized hesperetin then readily partitions into the corneal epithelial cells, from the stroma, because of its lipophilic nature (represented by $K_{10}[C_{UI}]_{St}$ of Eq. (6)). In contrast to the A–B direction, wherein the drug does not easily partition out from the epithelial layers into the stroma, in this case, because of higher log P, diffusivity will be high and overall

$$K_{10}[C_{UI}]_{St} \gg K_3\,[C_{UI}]_{Ep} \quad (8)$$

From the epithelial cells, drug partitioning into the receiver chamber will be facilitated by HP-β-CD or Tween® 80, present in the receiver solution (represented by $K_{12}[C_{UI}]_{Ep}$ of Eq. (6)). Moreover, the paracellular transport of hesperetin across the corneal epithelium in the B–A direction (represented by $K_{11}[C_I]_{St}$ of Eq. (6)) could also be significantly higher than that in the A–B direction because of the structural organization of the tight junctions (Sreeraj et al., 2003). Thus,

$K_{11}[C_I]_{St} \gg K_2[C_I]_{Dn}$ or

$K_{11}[C_I]_{Dn} \gg K_2\,[C_I]_{Dn}$ (refer to Eq. (7))

This is also consistent with the report from Pezron et al. (2002), wherein the authors observed a higher flux of zinc insulin in the B–A direction compared to A–B direction across Calu-3 cell monolayers. It was found that efflux by a transporter (P-gp), enzymatic degradation or the abundant insulin transporters on the basolateral side was not responsible for this asymmetric transport of insulin. The authors hypothesized that at the apical surface diffusion of insulin monomers is restricted by the presence of tight junction complexes, however, on the basolateral side insulin oligomers can diffuse into the intercellular spaces freely and dissociate and diffuse readily as monomers to the apical surface.

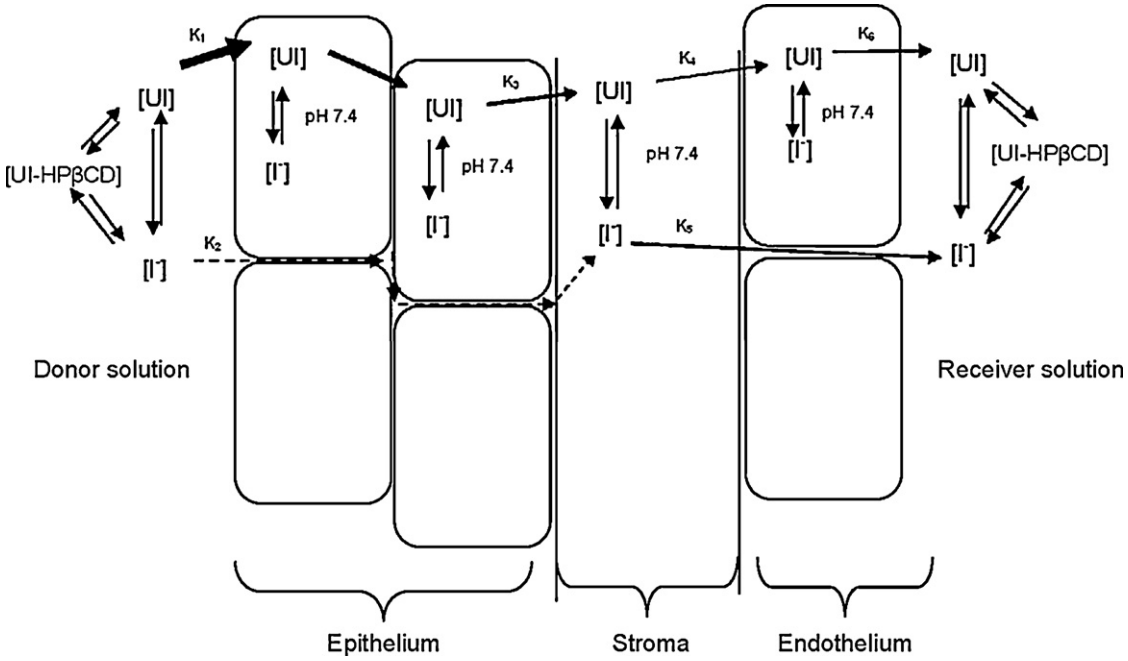

Fig. 6. Schematic representation of the transport of hesperetin across rabbit corneal layers in the apical to basolateral (A–B) direction. Thicker arrows denote the higher flux.

Considering better transcellular and paracellular diffusion rates in the B–A direction, the overall permeability in the B–A direction is greater. Differently stated, when hesperetin is diffusing in the B–A direction, the stroma is exposed to higher drug concentrations, thus narrowing down the diffusion path length by acting as a donor. On the other hand, in the A–B direction, the stroma holds relatively much lower fractions of hesperetin because of the larger barrier role of the epithelial cell layer in this case. Thus, low drug flux is observed in this direction. This hypothesis explaining the asymmetrical transcorneal diffusion of hesperetin is consistent with the reports of Schultz, which documents that passive asymmetric transport through the biological membranes is possible and that this could be attributed to the structural heterogeneity of the biological membrane (Schultz, 1971).

When the donor solution pH was decreased to pH 6, however, transcellular diffusion of hesperetin in the A–B direction increased dramatically (4.5-fold increase) due to a significantly higher concentration gradient of the unionized species. As a result more drug partitioned into the corneal epithelium and thus into the stroma and thus higher net diffusion in the A–B direction was observed. Moreover, unionized (uncharged) hesperetin molecules would demonstrate better paracellular diffusion characteristics

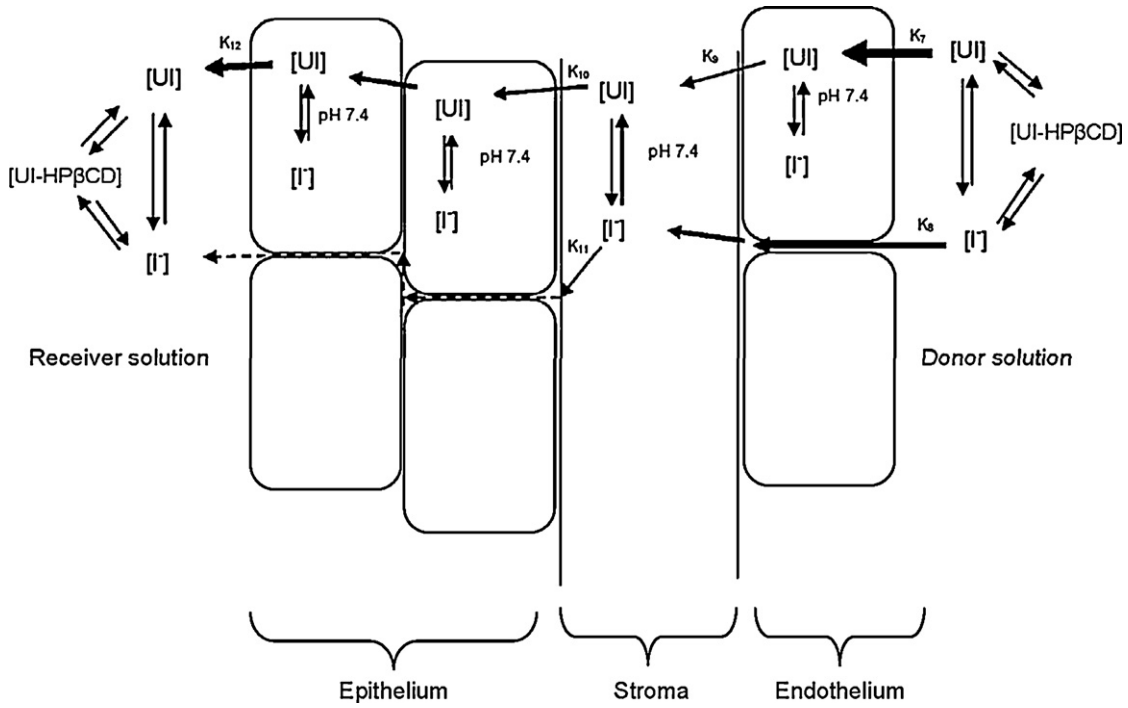

Fig. 7. Schematic representation of the transport of hesperetin across rabbit corneal layers in the basolateral to apical (B–A) direction. Thicker arrows denote the higher flux.

than the negatively charged species (Schanker, 1962). Thus, in the A–B direction, with the donor solution at pH 6, both transcellular as well as paracellular diffusion rates would increase.

On the other hand, when the donor solution was at pH 6, the B–A transport increased less markedly (1.5-fold) since trans-endothelial diffusion of hesperetin was anyway higher to start with. The slight increase observed would be because of increased transcellular diffusion of the unionized form and also improved paracellular diffusion of the unionized hesperetin molecule (both across endothelial and epithelial cell junctions). On the whole, transcellular diffusion rates would overshadow the paracellular diffusion component of hesperetin in the unionized state. Consequently A–B and B–A transport becomes equal when the donor solution pH is maintained at pH 6, i.e. the molecule exists in the unionized state.

It also appears that the composition of the transport medium could significantly affect the transcorneal transport symmetry. The difference between the A–B and B–A flux was significantly greater when HP-β-CD was used as the solubilizer. Considering the geometrical configuration, number of hydrogen bonding sites and the molecular weight of HP-β-CD, there is very little chance that HP-β-CD could penetrate into the stroma from the basolateral side. On the other hand the ability of Tween® 80 to diffuse into the stroma through the endothelial cells may be much greater because of its comparatively linear structure. Presence of a solubilizer in the stroma would significantly enhance $K_3[C_{UI}]_{Ep}$, and thus decrease the difference between the A–B and B–A diffusion rates. At 0.25% (w/v) the concentration of Tween® 80 generated in the stroma would be significantly lower than that obtained with 0.5% Tween® 80. Consequently, with 0.25% Tween® 80 a greater directional diffusion was observed compared to that with 0.5% Tween® 80. There could be an argument that at higher surfactant concentrations the biological membranes would be damaged. To check for this ACV, a molecule that traverses the corneal membrane primarily by diffusion across the paracellular pathway was included as an internal marker. In the same experimental set-up, while ACV demonstrated symmetrical transport across the cornea, hesperetin demonstrated asymmetrical transport. This demonstrates that a change in corneal integrity was not responsible for the directionality in the observed transcorneal permeation of hesperetin. Moreover, a decrease in the overall transcorneal hesperetin flux, at 0.5% Tween® 80, further indicates lack of surfactant induced membrane damage.

In conclusion, hesperetin is capable of permeating across the corneal tissue but exhibits asymmetric transport with the permeability in the A–B direction being significantly lower than that in the B–A direction. Unique structural features of the cornea and the transport medium components and solution pH, rather than the involvement of influx/efflux transporters, are probable reason behind the higher corneal permeability of the drug in the B–A direction.

Acknowledgments

This project was supported in part by Grant Numbers, P20RR021929 from the National Center for Research Resources (NIH/NCRR) and EY018426-02 from the National Eye Institute (NIH/NEI). The content is solely the responsibility of the authors and does not necessarily represent the official views of the National Center for Research Resources or the National Eye Institute, National Institutes of Health.

References

Aranganathan, S., Panneer Selvam, J., Nalini, N., 2009. Hesperetin exerts dose dependent chemopreventive effect against 1,2-dimethyl hydrazine induced rat colon carcinogenesis. Invest. New Drugs 27, 203–213.

Aranganathan, S., Selvam, J.P., Nalini, N., 2008. Effect of hesperetin, a citrus flavonoid, on bacterial enzymes and carcinogen-induced aberrant crypt foci in colon cancer rats: a dose-dependent study. J. Pharm. Pharmacol. 60, 1385–1392.

Brand, W., Padilla, B., Van Bladeren, P.J., Williamson, G., Rietjens, I.M., 2010. The effect of co-administered flavonoids on the metabolism of hesperetin and the disposition of its metabolites in Caco-2 cell monolayers. Mol. Nutr. Food Res., doi:10.1002/mnfr.200900183.

Brand, W., Van Der Wel, P.A., Rein, M.J., Barron, D., Williamson, G., Van Bladeren, P.J., Rietjens, I.M., 2008. Metabolism and transport of the citrus flavonoid hesperetin in Caco-2 cell monolayers. Drug Metab. Dispos. 36, 1794–1802.

Chiou, G.C., Xu, X.R., 2004. Effects of some natural flavonoids on retinal function recovery after ischemic insult in the rat. J. Ocul. Pharmacol. Ther. 20, 107–113.

Chiu, Y.Y., Higaki, K., Neudeck, B.L., Barnett, J.L., Welage, L.S., Amidon, G.L., 2003. Human jejunal permeability of cyclosporin A: influence of surfactants on P-glycoprotein efflux in Caco-2 cells. Pharm. Res. 20, 749–756.

Choi, E.J., 2008. Antioxidative effects of hesperetin against 7,12-dimethylbenz-(a)anthracene-induced oxidative stress in mice. Life Sci. 82, 1059–1064.

Choi, E.J., Ahn, W.S., 2008. Neuroprotective effects of chronic hesperetin administration in mice. Arch. Pharm. Res. 31, 1457–1462.

Galati, E.M., Monforte, M.T., Kirjavainen, S., Forestieri, A.M., Trovato, A., Tripodo, M.M., 1994. Biological effects of hesperidin, a citrus flavonoid. (Note I): antiinflammatory and analgesic activity. Farmaco 40, 709–712.

Garg, A., Garg, S., Zaneveld, L.J., Singla, A.K., 2001. Chemistry and pharmacology of the Citrus bioflavonoid hesperidin. Phytother. Res. 15, 655–669.

Hirata, A., Murakami, Y., Shoji, M., Kadoma, Y., Fujisawa, S., 2005. Kinetics of radical-scavenging activity of hesperetin and hesperidin and their inhibitory activity on COX-2 expression. Anticancer Res. 25, 3367–3374.

Hwang, S.L., Yen, G.C., 2008. Neuroprotective effects of the citrus flavanones against H_2O_2-induced cytotoxicity in PC12 cells. J. Agric. Food Chem. 56, 859–864.

Kobayashi, S., Tanabe, S., Sugiyama, M., Konishi, Y., 2008. Transepithelial transport of hesperetin and hesperidin in intestinal Caco-2 cell monolayers. Biochim. Biophys. Acta 1778, 33–41.

Majumdar, S., Hingorani, T., Srirangam, R., 2010. Evaluation of active and passive transport processes in corneas extracted from preserved rabbit eyes. J. Pharm. Sci. 99, 1921–1930.

Majumdar, S., Srirangam, R., 2009. Solubility, stability, physicochemical characteristics and in vitro ocular tissue permeability of hesperidin: a natural bioflavonoid. Pharm. Res. 26, 1217–1225.

Mannermaa, E., Vellonen, K.S., Urtti, A., 2006. Drug transport in corneal epithelium and blood–retina barrier: emerging role of transporters in ocular pharmacokinetics. Adv. Drug Deliv. Rev. 58, 1136–1163.

Mertens-Talcott, S.U., De Castro, W.V., Manthey, J.A., Derendorf, H., Butterweck, V., 2007. Polymethoxylated flavones and other phenolic derivates from citrus in their inhibitory effects on P-glycoprotein-mediated transport of talinolol in Caco-2 cells. J. Agric. Food Chem. 55, 2563–2568.

Paysant, J., Sansilvestri-Morel, P., Bouskela, E., Verbeuren, T.J., 2008. Different flavonoids present in the micronized purified flavonoid fraction (Daflon 500 mg) contribute to its anti-hyperpermeability effect in the hamster cheek pouch microcirculation. Int. Angiol. 27, 81–85.

Pezron, I., Mitra, R., Pal, D., Mitra, A.K., 2002. Insulin aggregation and asymmetric transport across human bronchial epithelial cell monolayers (Calu-3). J. Pharm. Sci. 91, 1135–1146.

Prausnitz, M.R., Noonan, J.S., 1998. Permeability of cornea, sclera, and conjunctiva: a literature analysis for drug delivery to the eye. J. Pharm. Sci. 87, 1479–1488.

Resnikoff, S., Pascolini, D., Etya'ale, D., Kocur, I., Pararajasegaram, R., Pokharel, G.P., Mariotti, S.P., 2004. Global data on visual impairment in the year 2002. Bull. World Health Org. 82, 844–851.

Schanker, L., 1962. Passage of drugs across body membranes. Pharmacol. Rev. 14, 501–530.

Schultz, J.S., 1971. Passive asymmetric transport through biological membranes. Biophys. J. 11, 924–943.

Serra, H., Mendes, T., Bronze, M.R., Simplicio, A.L., 2008. Prediction of intestinal absorption and metabolism of pharmacologically active flavones and flavanones. Bioorg. Med. Chem. 16, 4009–4018.

Sreeraj, M., Mitra, A., Patrick, M., 2003. Ophthalmic Drug Delivery Systems. Marcel Dekker Inc.

Tommasini, S., Calabro, M.L., Stancanelli, R., Donato, P., Costa, C., Catania, S., Villari, V., Ficarra, P., Ficarra, R., 2005. The inclusion complexes of hesperetin and its 7-rhamnoglucoside with (2-hydroxypropyl)-beta-cyclodextrin. J. Pharm. Biomed. Anal. 39, 572–580.

Vellonen, K.S., Mannermaa, E., Turner, H., Hakli, M., Wolosin, J.M., Tervo, T., Honkakoski, P., Urtti, A., 2010. Effluxing ABC transporters in human corneal epithelium. J. Pharm. Sci. 99, 1087–1098.